iScience

CellPress
OPEN ACCESS

Article

Encoded and updated spatial working memories share a common representational format in alpha activity

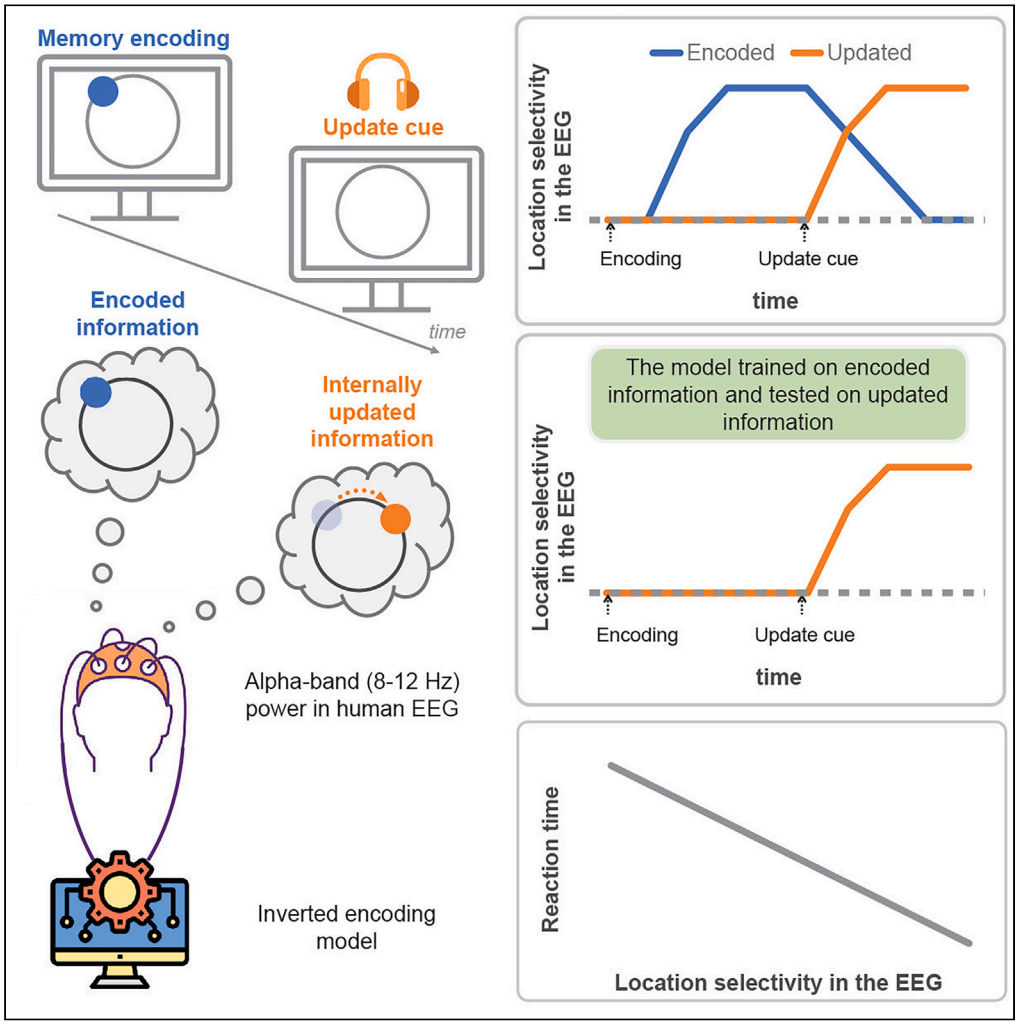

Eren Günseli, Joshua J. Foster, David W. Sutterer, Lara Todorova, Edward K. Vogel, Edward Awh

gunseli.eren@gmail.com

Highlights

Novel method to track voluntary transformations of mental representations

Alpha activity dynamically tracks updates in spatial working memory

The tracked updating rate predicts response times

Encoded and updated working memories share a common representational format

Günseli et al., iScience 27, 108963
February 16, 2024 © 2024
https://doi.org/10.1016/j.isci.2024.108963

iScience

CellPress
OPEN ACCESS

Article

Encoded and updated spatial working memories share a common representational format in alpha activity

Eren Günseli,[1,5,*] Joshua J. Foster,[2,3] David W. Sutterer,[4] Lara Todorova,[1] Edward K. Vogel,[2,3] and Edward Awh[2,3]

SUMMARY

Working memory (WM) flexibly updates information to adapt to the dynamic environment. Here, we used alpha-band activity in the EEG to reconstruct the content of dynamic WM updates and compared this representational format to static WM content. An inverted encoding model using alpha activity precisely tracked both the initially encoded position and the updated position following an auditory cue signaling mental updating. The timing of the update, as tracked in the EEG, correlated with reaction times and saccade latency. Finally, cross-training analyses revealed a robust generalization of alpha-band reconstruction of WM contents before and after updating. These findings demonstrate that alpha activity tracks the dynamic updates to spatial WM and that the format of this activity is preserved across the encoded and updated representations. Thus, our results highlight a new approach for measuring updates to WM and show common representational formats during dynamic mental updating and static storage.

INTRODUCTION

Working memory (WM) is the ability to store and manipulate information to guide behavior in ongoing tasks.[1] WM plays a central role in a wide range of cognitive tasks. Indeed, successful WM capacity predicts higher-order cognitive skills such as reasoning, problem-solving, and general fluid intelligence.[2–6] Since we live in a dynamic environment, we must transform or update information stored in WM so that it reflects the current state of our environment. For example, while driving, we intermittently check the rearview mirror. Between each glance at the mirror, we estimate the position of the car approaching from behind based on its position and speed the last time we checked the mirror. In other words, we must endogenously update its location in WM. If the car in front of us stops abruptly and we have to make a rapid decision (e.g., whether to apply the brakes hard or switch lanes) without the time to check the rear window, we can rely on this internally generated spatial WM representation. Given the important role of WM transformation in daily life, discovering how updated memories are represented is crucial for understanding the nature of WM.

Recent work has shown that rhythmic activity in the alpha frequency band (8–12 Hz) enables precise decoding of visual information during perception,[7,8] sustained storage in WM,[8,9] long-term memory retrieval,[10] and mental imagery.[7] Moreover, cross-temporal analyses have shown that the same patterns of alpha-band activity generalize across perception and mental imagery suggesting that they rely on common neural representations.[7] These studies focused on representations of information as they were encoded from the environment. However, as in the driving example provided above, we must often mentally transform representations stored in WM.

In this study, we ask two related questions. First, does alpha-band activity track the updates to spatial representations in WM? If so, do *updated* spatial working memories share a common representational format with representations of encoded visual input? An alternative possibility is that internally directed updates of spatial representations may alter the format of the representation. For instance, Yu et al. (2020)[11] found evidence for strong transformations (i.e., "rotations") of the format of neural representations when they were moved in and out of the focus of attention. Moreover, past work has found shifts in the frequency bands containing information about prioritized and unprioritized memory representations,[12] which raises the possibility that updated and encoded WM representations might be indexed by activity in different frequency bands. Thus, we examined whether dynamic *updating* of a representation in spatial WM has similar effects as when an observer voluntarily switches attention from one item to another. It is important to note that here we use the term updating to refer to endogenously generating a novel representation (i.e., transformation) instead providing participants with novel information to replace existing representation (i.e., replacement), both of which can be referred to as updating across studies (cf.[13,14]).

To examine these questions, we used an inverted encoding model (IEM) applied to alpha activity measured with EEG to reconstruct the contents of spatial WM in a task that required subjects mentally update a stored position to a new position (Figure 1). First, we tested whether

[1]Department of Psychology, Sabancı University, Istanbul, Turkey
[2]Department of Psychology, University of Chicago, Chicago, IL, USA
[3]Institute for Mind and Biology, University of Chicago, Chicago, IL, USA
[4]Department of Psychology, University of Tennessee, Knoxville, TN, USA
[5]Lead contact
*Correspondence: gunseli.eren@gmail.com
https://doi.org/10.1016/j.isci.2024.108963

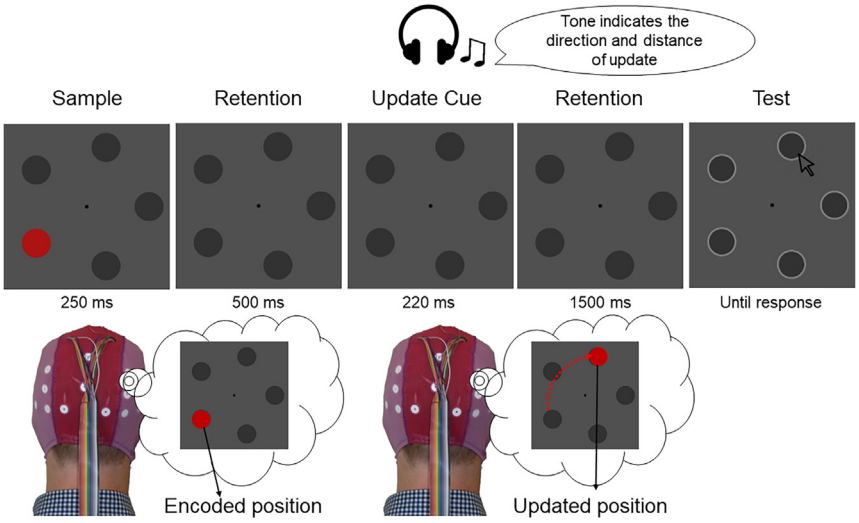

Figure 1. The experimental procedure in Experiment 1

Subjects were presented with the initial "encoded" position to be held in working memory. After a retention interval, they updated the position in their mind based on an auditory update cue that indicated the direction and distance of the update via its pitch and repetition. For example, two beeps with a high pitch indicated a clockwise two-step movement. At the end of the trial, subjects used a mouse click to indicate which placeholder contained the updated position. Experiment 2 was identical except the sample display was 150 ms, the second retention interval was 1000 ms, and the response was made by the gaze position recorded with an eye tracker instead of a mouse click.

the alpha-band activity would index dynamically shifting representations in spatial WM. Second, by training the IEM model trained on the EEG signal *before* the update and testing it for the WM content *after* the update, we examined whether there is a common format for updated and encoded representations in spatial WM.

We found that the contents of spatial WM could be reconstructed based on the topographic distribution of alpha-band power both for encoded and updated working memories. Moreover, when the IEM model was trained on the alpha activity before updating, we were able to successfully reconstruct the WM content after mental updating, demonstrating that encoded and updated spatial working memories share a common representational format. Finally, these patterns of alpha activity were sensitive to the efficiency with which subjects could indicate the updated location, both between individuals (Experiment 1) and across trials within individuals (Experiment 2). These findings highlight a new approach for tracking the dynamic updating of representations in visual WM in a time-resolved manner. Moreover, they show a clear correspondence between the representational formats of storing encoded and internally generated WM representations.

RESULTS

Behavior

Behavioral results show that subjects were able to perform the task with high accuracy in both experiments. The grand average accuracy was 97.1% (*SD* = 2.6%) in Experiment 1 and 93.9% (*SD* = 4.9%) in Experiment 2. In Experiment 1, where subjects reported the updated location with a mouse click, RTs were 911 ms average (*SD* = 364 ms) on. In Experiment 2, where subjects responded by making a saccade to the remembered location, response times were much faster: 357 ms on average (*SD* = 74 ms).

EEG

Alpha-band scalp topography tracks updated content in spatial WM

Figure 2 shows the CTFs, and Figure 3 shows the slopes of the CTFs for both experiments. Our analysis showed that the encoded memory position was actively maintained throughout the initial retention interval until the update cue for both experiments, as alpha-band power CTFs revealed a sustained spatial selectivity during this interval. This finding replicates Foster et al. (2016) and shows that alpha-band scalp topography tracks the contents of spatial WM.

Importantly, the location selectivity for the *updated* position was also tracked in the alpha-band topography. It emerged following the update cue and was sustained until the test display. This result extends previous findings and shows that alpha-band topography can be used to reconstruct *updated* contents of spatial WM in addition to the non-updated contents. Moreover, the location selectivity was not due to a mere lateralization of alpha-band activity but rather reflected the precise location held and updated in WM, as each location channel's tuning profile was distinct from others (Figure S1).

Foster et al. (2016)[8] found that reconstruction of the contents of spatial WM is specific to the alpha band and is not reflected in other frequency bands. Accordingly, we next tested if the same range of frequency bands tracks the updated contents of WM.

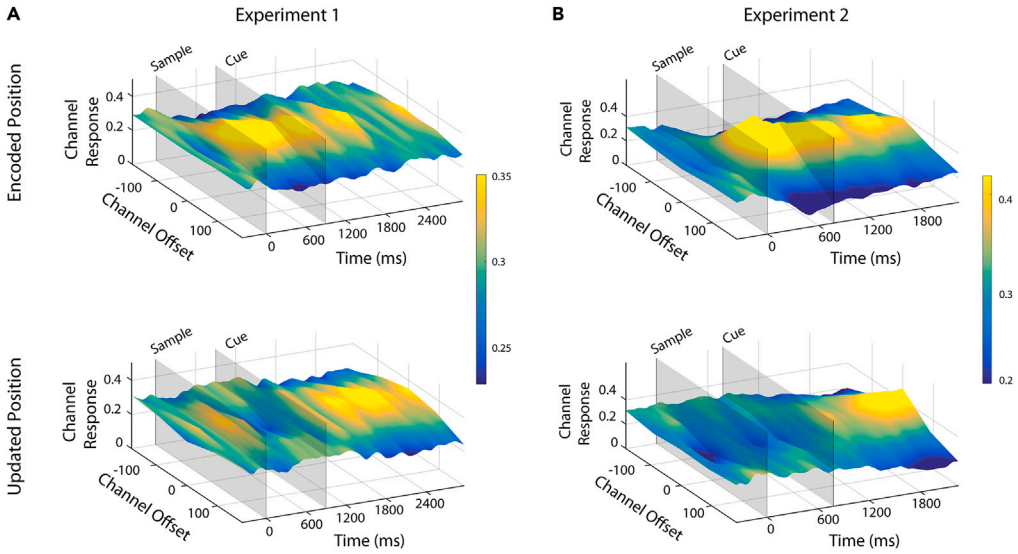

Figure 2. Channel tuning functions (CTFs)

The CTFs reconstructed using an inverted encoding model (IEM) on the alpha-band (8–12 Hz) power in the EEG signal provided time-resolved tracking of the encoded and updated positions both in (A) Experiment 1 and (B) Experiment 2. CTFs are shown separately for the encoded position (top row) and updated position (bottom row). The onset of sample and cue displays are shown with gray rectangles. Higher and yellower peaks in the CTFs indicate larger location selectivity in alpha-band power. In both experiments, alpha-band power showed location selectivity for the encoded position after the sample display and for the updated position after the update cue.

Updated and encoded working memories are both represented in the alpha-band activity

Previous studies found enhanced activity in the dorsolateral prefrontal cortex for updating vs. storage in WM using fMRI.[15–17] These results suggest that updating might require additional attentional resources compared to mere storage in WM. Moreover, past work has found shifts in the frequency bands representing information about prioritized and unprioritized memory representations.[12] This raises the possibility that updated and encoded WM representations might be indexed by activity in different frequency bands.

Accordingly, we examined whether updated representations in WM were represented within the same range of frequency bands as the positions cued by external stimuli. To test this, we calculated CTFs across frequency bands ranging from 4 Hz to 50 Hz. For both experiments, location selectivity was mainly restricted to the alpha-band, both for the encoded and updated position (Figure 4). There are three exceptions to this.

First, early in the trial, location selectivity was also present in theta band activity (~4–7 Hz). This result is consistent with previous work that shows early (0–500 ms) location selectivity in the theta band for spatial WM representations (e.g., Foster et al., 2016).[8] Importantly,

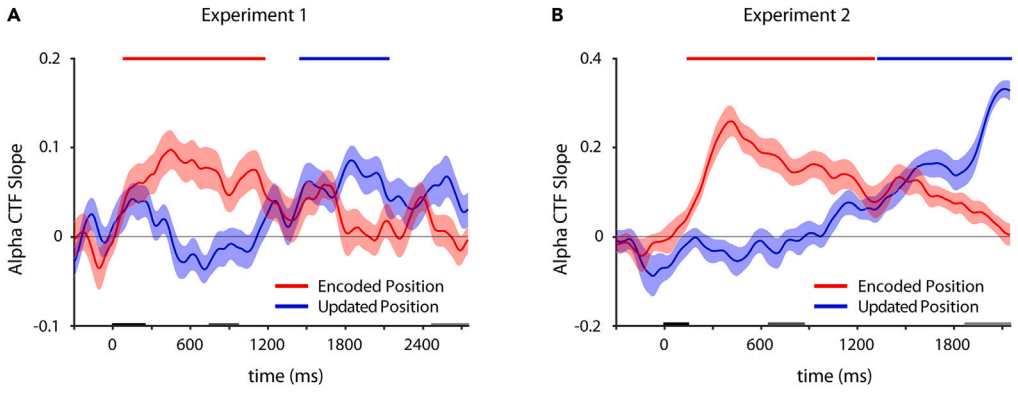

Figure 3. Location selectivity quantified via the alpha-band (8–12 Hz) CTF slope

(A and B) Location selectivity in the EEG that is quantified by the alpha-band (8–12 Hz) CTF slopes for (A) Experiment 1 and (B) Experiment 2, shown in different colors for the encoded and updated positions. The markers along the top of the panes, shown in the same colors as the main CTF slopes, indicate the time points at which the CTF slope was reliably above chance as indicated by a cluster-based permutation test against a randomly permuted sample ($p < 0.05$; two-tailed). Shaded error bars show the bootstrapped standard error of the mean.

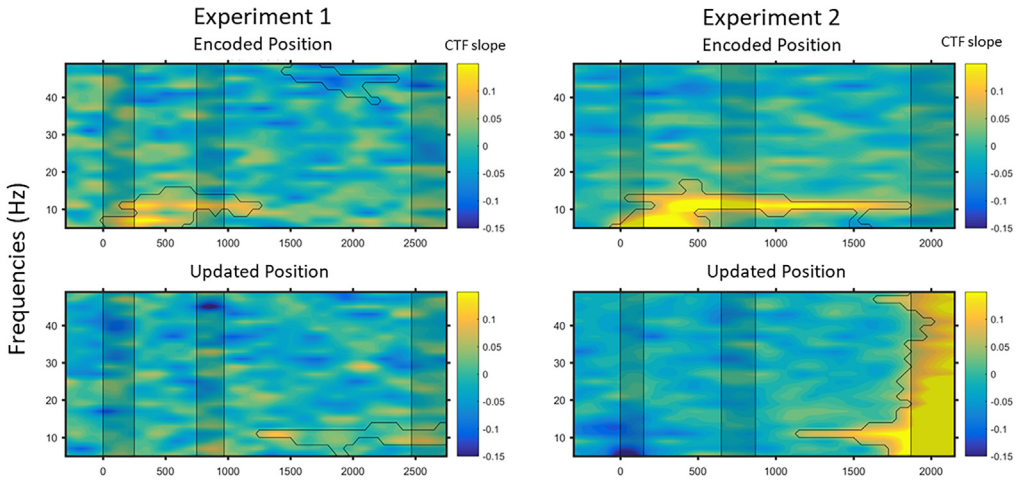

Figure 4. Location selectivity across frequencies

Location selectivity (i.e., CTF slope) in the EEG across frequency bands ranging from 4 Hz to 50 Hz quantified as CTF slopes for Experiment 1 (left) and Experiment 2 (right) shown in separate panels for encoded (top) and updated positions (bottom). The black lines indicate the time-frequency bands at which the CTF slope was reliably above chance as indicated by a cluster-based permutation test against a randomly permuted sample ($p < 0.05$; two-tailed). Shaded rectangles show the duration the sample, update cue, and the probe were presented, respectively.

this low-frequency location selectivity was not sustained either in the present work or in Foster et al. (2016),[8] which suggests that it likely represents the initial encoding of stimuli instead of storage in WM. In line with this, there was no theta-band selectivity for the updated position. Second, only in Experiment 1, there was a significant cluster approximately between 1500 and 2300 ms in a high-frequency band (~40–50 Hz). However, this cluster had a negative CTF slope indicating a location 'unselectivity' for the encoded position. This result is likely a false positive because the same pattern was not observed in Experiment 2, which had higher power due to a larger number of trials. Third, in Experiment 2, right before the probe onset, there was location selectivity across all frequencies. Given that in Experiment 2, participants indicated their response by moving their eyes to the placeholder of the updated position, we suggest that this broad-band location selectivity specific to the updated position reflects eye-movement preparation-related activity and not WM storage. In line with this, such frequency unspecific reconstruction was not observed in Experiment 1. Moreover, only the alpha-band location selectivity was common in both experiments, reaching significance approximately 300 ms after the offset of the update cue, which is approximately 550 ms before the broadband selectivity. Thus, we conclude that spatial WM representations were restricted to the alpha-band activity both for stationary and updated contents.

Updated and encoded working memories share a common representational format

Our results above show that alpha-band topography tracks both the encoded and updated contents of spatial WM. Next, we asked whether encoded and updated working memories are represented in a common representational format. Although our analyses so far have shown that encoded and updated working memories are represented by alpha activity, it remains to be seen whether encoded and updated working memories share a common representational format because each CTF was trained and tested separately for encoded and updated working memories.

To test whether updated and encoded working memories share a common representational format, we trained the IEM for the encoded position during the initial retention interval and tested the IEM for the updated position at each time point. Thus, the training of the IEM was blind to the information regarding the position of the updated content. We hypothesized that this cross-training should demonstrate location selectivity only if the storage of encoded and updated contents in spatial WM relies on an overlapping representational format as reflected in alpha-band power scalp topography. On the other hand, if the storage of updated contents relies on a different pattern of neural activity than the initial storage in WM, then training the IEM on the encoded position should not reveal location selectivity for the updated position.

For both experiments, training the IEM based on the EEG activity pattern for the encoded WM content prior to the update cue and testing it for the updated content at each time point produced an accurate and reliable reconstruction of the updated content following the update cue (Figure 5). This result suggests that the storage of the encoded and updated content in spatial WM share an overlapping neural representational format.

Alpha-band scalp topography for the updated content predicts behavior

To examine whether alpha band activity was linked with behavior, we tested whether the selectivity of the CTF tracking the updated representation was correlated with the reaction time for reporting the updated position. For this test, we used a within-subjects correlation in Experiment 1 that contained a high number of trials and a between-subjects correlation in Experiment 2 that contained a high number of participants. Indeed, the average CTF slope for the updated position after the update cue (i.e., from the offset of the update cue until the

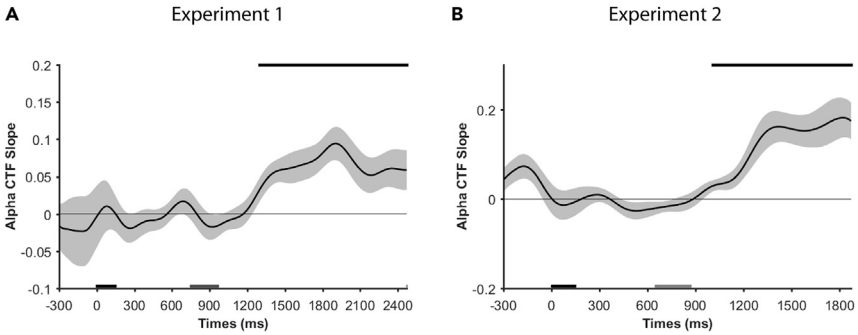

Figure 5. Overlapping neural representations for the encoded and updated positions

CTF slope for the updated position was obtained by cross-training the IEM based on the encoded position prior to the cue and testing it for the updated position at each time point for (A) Experiment 1 and (B) Experiment 2. Shaded error bars show the bootstrapped standard error of the mean. The black markers along the top of the panes indicate the time points at which the CTF slope was reliably above chance as indicated by a cluster-based permutation test against a randomly permuted sample ($p < 0.05$; two-tailed). The above chance reconstruction of the updated position using the encoded position labels suggests that updated and encoded spatial WM contents have overlapping neural representations.

onset of the test display) predicted the average RT across subjects, $R^2 = 0.25$, $p = 0.005$ (Figure 6A). There was no CTF slope-accuracy correlation, presumably because of the low variance in accuracy data ($M = 97.1\%$. $SD = 2.6\%$). Interestingly, this correlation was observed in Experiment 1 even though subjects were not told to prioritize speed when they made their manual responses.

In Experiment 2, by contrast, subjects were instructed to move their eyes to the updated position as quickly as they could after the onset of the test display, yielding much shorter response latencies. In addition, we collected twice the number of trials in Experiment 2 compared to Experiment 1, providing adequate data to look at CTF selectivity across fast and slow trials in a within-subject analysis. Thus, the data were divided based on a median split of saccade latencies. First, an IEM with each of the three blocks containing an equal number of above-median RT (i.e., slow response) and below-median RT (i.e., fast response) trials was used to train the model. Then, location selectivity was tested separately for fast and slow response trials, resulting in separate CTFs. Lastly, as in Experiment 1, we averaged the CTF slopes for the updated position following the update cue. The average CTF slope for the updated position was larger in fast response trials (*Mean Response Time* = 202.3 ms; *SD* = 26.0 ms), $M = 0.08$ ($SD = 0.08$), compared to slow response trials (*Mean Response Time* = 510.3 ms; *SD* = 130.5 ms), $M = 0.04$ ($SD = 0.06$), $t(17)$, 34.01, $p < 0.0001$ (Figures 6B and 6C). Together, these results suggest that the active storage of the updated content in WM, as indexed by the larger CTF slope, predicted faster eye movements to the updated position.

Eye movements do not account for the location selectivity in the EEG signal

Trials with ocular artifacts were removed prior to any analysis. However, there were subtle but systematic eye movements remaining (Figure S2). To test the influence of these eye movements on our CTF location selectivity results, we repeated our main analysis using recorded eye positions to determine the position bins in the IEM. We performed this analysis for Experiment 2 because for this experiment we had reliable eye-tracking data for all participants and almost every trial, as trials with eye movements were aborted and repeated.

The location selectivity, derived from the analysis using recorded eye positions was a few times smaller in magnitude and shorter in duration (Figure S3). To quantify this difference, we compared the mean CTF slopes computed based on gaze positions (Figure S3A) and actual positions (Figure S3B). For the encoded position during the first retention interval, the mean CTF slope was larger when computed using the actual encoded position ($M = 0.19$) compared to using the mean gaze position ($M = 0.05$), $t(17) = 7.25$, $p < 0.001$. Similarly, for the updated position during the second retention interval, the mean CTF slope was larger when computed using the actual updated position ($M = 0.09$) compared to using the mean gaze position ($M = 0.03$), $t(17) = 3.01$, $p = 0.008$. These results provide strong evidence that gaze position alone cannot account for the location tracking in our study.

DISCUSSION

The updating of WM representations is crucial for humans to successfully guide their behavior in a dynamic world. Here, we extended prior work that has shown that alpha activity tracks locations stored in WM,[8] showing that alpha activity also tracks the updating of locations stored in WM. Specifically, we show that alpha-band activity also indexes dynamic updating of representations in spatial WM, with spatially selective activity tracking the updated positions within several hundred milliseconds of the update cue. Successful reconstructions were specific to the alpha-band power for both updated and encoded representations. In addition, cross-training analyses showed that the format of alpha activity was similar across the updated and encoded positions. Specifically, training the IEM based on the *encoded* WM content before the update cue was sufficient to track the *updated* WM position from the subsequent phase of the trial. Finally, the location selectivity for the updated position in the EEG signal predicted which subjects reported that location the fastest (Experiment 1) and distinguished between fast and slow responses in a within-subject analysis (Experiment 2). Thus, these findings highlight a new approach for precisely tracking dynamic updates of spatial WM representations and reveal a common format of alpha activity for static and dynamic representations.

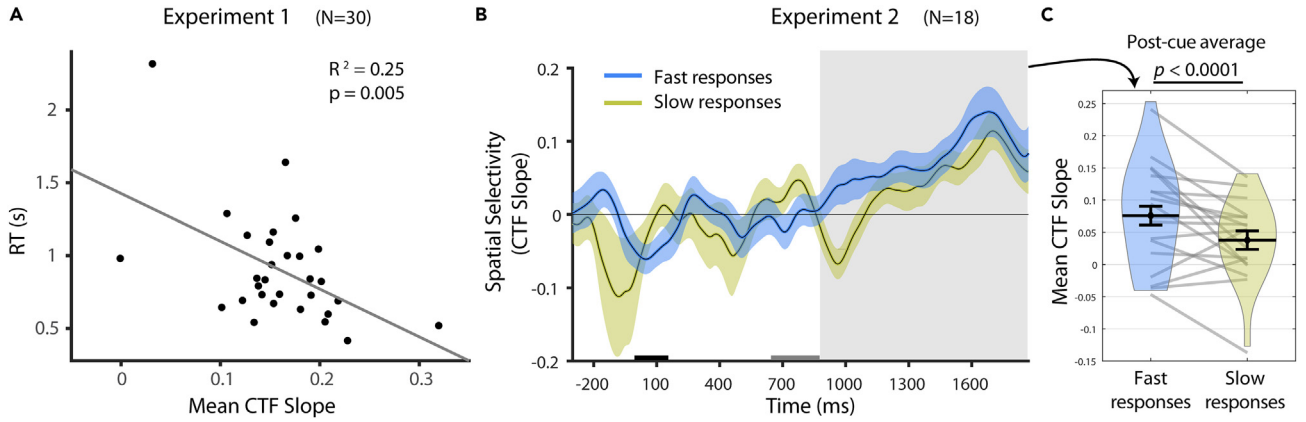

Figure 6. Higher location selectivity in the EEG predicted faster responses

(A) In Experiment 1, the mean CTF slope for the updated position following the update cue predicted average RT across subjects ($p = 0.005$).

(B) In Experiment 2, the CTF slope for the updated position across time points is shown separately for fast response (i.e., below-median RT) and slow response (above median RT) trials in different colors. The dark gray and light gray bars on the x axis indicate the timing of the sample and cue displays respectively. The big shaded gray region shows the 2nd retention interval, from the offset of the update cue until the onset of the test display, at which the average CTF slope for the updated position was calculated. Shaded error bars show the bootstrapped standard error of the mean.

(C) The average CTF slope during the 2nd retention interval (shown in the gray region in B) separately for fast response and slow response trials. Fast response trials had a larger CTF slope than slow response trials ($p < 0.0001$). The error bars show the standard error of the mean for data normalized for the between-subjects variance.

Recent evidence suggests that alpha-band activity in the EEG enables the tracking of visual information held in WM[8,9] and mental imagery.[7] In a mental imagery task, Xie et al. (2020)[7] provided an auditory recording of a word that represents an object (e.g., apple) that participants were instructed to visually imagine. A classifier was trained on the data when participants viewed the same objects on the screen and tested when participants were given auditory cues to imagine the objects. EEG activity in the alpha-band power provided successful decoding of object categories suggesting that alpha-band activity underlies the perception and mental imagination of information in visual WM. However, the mental imagery task always followed the perception task where individuals viewed the same images across dozens of trials. Thus, it is likely that individuals retrieved these images from long-term memory when instructed to imagine them, as opposed to internally generating mental imagery. Moreover, the cross-decoding in Xie et al. (2020)[7] was between perception and imagery, while we obtained it between the static storage of encoded representations in WM and later dynamically updated representations via mental imagery. Lastly, previous studies were focused on static representations in WM, either based on a visual presentation[8,9] or auditory retrieval cues.[7] Thus, a key extension offered by the present work is the demonstration of overlap in the format of alpha activity during WM and imagery that is maintained during the dynamic updates of spatial representations that were required by a mental updating task.

Updating information has been previously studied using fMRI in the domain of mental imagery. These studies showed that motor areas, parietal cortex, and early visual areas are involved in mental rotation and updating of information in VWM.[18–23] More recently, MVPA was used to investigate the brain regions that represent the contents of mental rotation. Subjects were given an orientation or a shape to remember and then they rotated the orientation in their mind based on rotation cues that indicated direction and degrees of rotation (e.g., clockwise 60°). The results showed that early visual areas (V1-V4) stored the encoded orientation and also, following the rotation cue, the rotated orientation.[24,25] Moreover, Albers et al. (2013)[24] obtained cross-decoding between training on WM retention and testing on mental imagery. Thus, these studies provide evidence for a neural overlap for storing encoded and mentally updated representations in WM. However, given the differences in cognitive and neural mechanisms for representing object vs. spatial information in WM both during storage and updating,[9,26–35] it remained an open question whether encoded and updated *spatial* information in WM also rely on overlapping neural representations. In addition, oscillatory activity measured with EEG may tap into distinct aspects of WM maintenance than does BOLD activity measured with functional MRI. Thus, our demonstration that oscillatory activity indexes the storage of both encoded and updated representations in WM provides a strong complement to the previous work.

We found evidence for overlapping representational formats for encoded and updated spatial WM representations. Specifically, we obtained location selectivity when cross training the IEM on the average activity based on the encoded position before the update cue and testing it for the updated position at each time point. The location selectivity obtained via this cross-training emerged earlier compared to training and testing the IEM at each time point. There are two explanations for this earlier emergence of location selectivity that are not mutually exclusive. First, a model trained by averaging across a wide time window might have been more robust compared to training for each time point, increasing the statistical power. Second, the earlier emergence of selectivity for the updated position might be meaningful in terms of the underlying cognitive mechanisms. Although memories are reinstated by reactivating patterns of activity that belong to initial encoding, memories also transform over time, being represented in distinct but predictable neural patterns and brain regions.[36–40] Thus, it is possible that first, the updated position starts being represented in a format that overlaps with the encoded memory, and then a parallel

updated format emerges later in the retention interval. Future studies that are better suited to disentangle the overlap and dissociation between encoded and updated memories can explore this possibility.

The term mental imagery has been used to refer to two different cognitive operations. One is acting on representations in a way to transform them, such as mental rotation.[15,16,24,25] This type of mental imagery is the focus of the present manuscript. The term mental imagery has also been used to refer to recalling and imagining previously learned stimuli.[7,41–44] Overall, these studies showed that mental imagery, whether updating or retrieval based, is established via neural activation of early perceptual visual regions as WM storage does (but see[21]). Moreover, recent MVPA studies showed that not only the level of activity but also patterns of activity in these regions overlapped in imagery and perception.[24,25] However, all but one of these studies investigated mental imagery in the visual domain, using oriented lines, faces, objects, or abstract shapes. The only study that investigated the updating of spatial information used univariate methods.[16] Although this study showed that there was an overlap in the brain regions that were active during storage and updating in the spatial domain, it was not able to show whether the information content was represented in overlapping brain regions. Even so, representations in the same brain areas do not demonstrate overlapping representations.[11,45] Thus, our results provide the first evidence of overlapping neural representations of WM storage and mental imagery in the spatial domain.

The CTF slope for the updated position during the 2nd retention interval predicted RT across subjects (Experiment 1), with increased selectivity predicting faster manual report of the updated position. Given that subjects were not instructed to respond as quickly as possible in this experiment, we speculate that this finding may reflect strategic differences between subjects regarding the timing of their mental updating. Some subjects may have adopted a more prospective strategy of immediately shifting the representation to the cued position, while other subjects may have waited until closer to the end of the delay period to perform the update. Thus, we hypothesize that subjects who rotated early had more time to prepare their response before the test display was presented. Indeed, the switch to a speeded task in Experiment 2 was motivated by the correlation observed in Experiment 1. When subjects in Experiment 2 were explicitly instructed to respond as fast as possible, the average RT was ~3 times faster, and the standard deviation was 4.9 times smaller compared to Experiment 1 though this can be partly due to the faster nature of saccadic responses over mouse clicks. This difference in RT between the two experiments that differed in instructions suggests that the rate with which WM updating takes place can be adjusted based on incentives and strategies. This conclusion is consistent with a recent finding that showed the use of a prospective strategy in WM could be biased by task demands.[46] Having a large number of trials in Experiment 2 (almost double of Experiment 1) allowed an analysis across trials using a median split approach on RT. The location specificity for the updated content, as indexed by the CTF slope, was higher in fast RT trials than in slow RT trials. This result is in line with the between-subject correlation between average RT and average CTF slope in Experiment 1 and strengthens our conclusion that alpha activity tracks the temporal dynamics of WM updating.

The location information for the encoded position was evident not only before the update cue but also after the update cue for a few hundred milliseconds. The timing of this ongoing location selectivity for the encoded position overlapped with the emerging location selectivity for the updated position. We claim that there are three possible explanations for this overlap. First, the location selectivity could reflect the temporal smearing that emerges due to time-frequency decomposition.[47] Second, there might be variation across individuals such that some start and perform the update after the update cue. If so, averaging across trials would result in temporal smearing in location selectivity for the encoded and updated positions. Third, participants can store the initial encoded position as a reference while computing the updated position. Doing so would require simultaneously storing in WM both the encoded position and the updated position. While the noise in the EEG does not allow testing this possibility, it is an intriguing question to explore for studies that use measures with higher signal-to-noise such as intracranial recordings.

An interesting question that emerges from the present work is regarding the generalizability of alpha-based tracking of WM updates to the non-spatial domain. Alpha-band EEG topography has been reliably used to decode and reconstruct the contents of spatial memories.[8–10,48] Moreover, Bae & Luck (2018)[49] found that alpha-band topography can be used to decode the location but not orientations held in WM. This finding suggests that alpha-band activity in the EEG contains information about spatial but not non-spatial representations. However, contrary to this claim, Xie et al. (2020)[7] used alpha-band activity to decode object identities (e.g., apple, carrot, car) both during perception and retrieval-type imagery. Thus, a possibility that warrants investigation in future studies is that endogenous updates to WM representations can be tracked in alpha-band activity not only for spatial contents, as shown in the present study, but also for non-spatial contents.

Previous studies have shown a tight interweaving between spatial attention and spatial WM.[50–53] Observers orient attention toward locations held in WM[50] even when location is completely irrelevant to the memory task.[9] Thus, spatial attention typically provides a sensitive index of the locations that are currently stored in WM. Nevertheless, there is emerging evidence for a dissociation between spatial attention and WM. At times, spatial attention can be deployed to items that are not encoded into WM,[54] suggesting that spatial attention and WM gating could reflect distinct aspects of attentional control. Likewise, spatial attention and storage within WM can be modulated independently depending on anticipated task demands: First, items receive greater attention but equal WM activation when anticipated to be used in more difficult tasks[55] or to be more likely to be probed.[56] Second, previously studied items are more strongly activated but receive less attention when anticipating distractors at locations that overlap with memory locations.[57] Third, repeatedly stored items that are handed off to LTM are more strongly reactivated in WM without receiving more attention when anticipated to be used in a new task rule.[58] These findings demonstrate that WM storage can be dissociated from spatial attention. Thus, while tracking spatial attention has typically been a robust method for tracking the likely contents of WM, there is motivation for future work to examine how alternative signatures of storage in spatial WM will respond to the requirement to internally update those memory representations.

To conclude, we show that alpha activity precisely tracks the mental updating of spatial representations in WM. Furthermore, we found that encoded and updated representations in spatial WM are represented in a common representational format. Together, our results highlight a powerful approach for tracking the endogenous updating of online spatial memory representations.

Limitations of the study

While our study provides valuable insights into the role of alpha activity in tracking updates to dynamic WM updating and the overlap of the representation format for encoded and updated information, it is essential to acknowledge certain limitations. First, our experimental paradigm focused on spatial representations, and the generalizability of our findings to nonspatial WM contents remains an open question. Future research should explore whether alpha activity exhibits similar tracking capabilities for other types of WM representations. Additionally, the voluntary mental transformations assessed in our task may involve strategic variations among individuals, influencing the observed temporal dynamics. Exploring how individual differences in strategy affect memory representations and behavioral performance is an exciting area for future work.

STAR★METHODS

Detailed methods are provided in the online version of this paper and include the following:

- KEY RESOURCES TABLE
- RESOURCE AVAILABILITY
  - Lead contact
  - Materials availability
  - Data and code availability
- EXPERIMENTAL MODEL AND STUDY PARTICIPANT DETAILS
- METHOD DETAILS
  - Stimuli
  - Design and procedure
  - EEG recording
- QUANTIFICATION AND STATISTICAL ANALYSIS
  - Behavioral
  - Eye-tracking
  - Artifact rejection
  - Power analyses
  - Inverted encoding model of spatial position
  - Statistical analysis
  - EEG-behavior relationship
  - Eye bias control analysis

SUPPLEMENTAL INFORMATION

Supplemental information can be found online at https://doi.org/10.1016/j.isci.2024.108963.

ACKNOWLEDGMENTS

This work was supported by NIMH grant 2R01MH087214-06A1 to E.A. and E.K.V. We would like to thank Shannon Heald for creating the sound files used as the update cues, and Ariana Gale, Brendan Colson, Melanie Sykes, and Emily Xue for assisting with data collection.

AUTHOR CONTRIBUTIONS

Conceptualization: E.G., J.J.F., D.W.S., E.K.V., and E.A.; Data curation: E.G.; Formal Analysis: E.G., J.J.F., D.W.S., and L.T.; Funding acquisition: E.K.V. and E.A.; Methodology: E.G., J.J.F., D.W.S., and E.A.; Writing – original draft: E.G., J.J.F., D.W.S., E.K.V., and E.A.; Writing – review and editing: E.G., J.J.F., D.W.S., L.T., E.K.V., and E.A.

DECLARATION OF INTERESTS

The authors declare no competing interests.

DECLARATION OF GENERATIVE AI AND AI-ASSISTED TECHNOLOGIES IN THE WRITING PROCESS

During the preparation of the highlights and limitations of the study sections, the authors used ChatGPT 3.5 in order to obtain a brief and concise summary of key findings and limitations. After using this tool, the authors reviewed and edited the content as needed and take full responsibility for the content of the publication.

Received: June 23, 2023
Revised: August 8, 2023
Accepted: January 15, 2024
Published: January 17, 2024

REFERENCES

1. Baddeley, A., and Hitch, G. (1974). Working Memory. In Psychology of Learning and Motivation, G.H. Bower, ed. (Academic Press), pp. 47–89.
2. Carpenter, P.A., Just, M.A., and Shell, P. (1990). What one intelligence test measures: A theoretical account of the processing in the Raven Progressive Matrices Test. Psychol. Rev. *97*, 404–431.
3. Chow, M., and Conway, A.R.A. (2015). The scope and control of attention: Sources of variance in working memory capacity. Mem. Cognit. *43*, 325–339.
4. Engle, R.W., Tuholski, S.W., Laughlin, J.E., and Conway, A.R.A. (1999). Working memory, short-term memory, and general fluid intelligence: a latent-variable approach. J. Exp. Psychol. Gen. *128*, 309–331.
5. Fukuda, K., Vogel, E., Mayr, U., and Awh, E. (2010). Quantity, not quality: the relationship between fluid intelligence and working memory capacity. Psychon. Bull. Rev. *17*, 673–679.
6. Kane, M.J., and Engle, R.W. (2002). The role of prefrontal cortex in working-memory capacity, executive attention, and general fluid intelligence: An individual-differences perspective. Psychon. Bull. Rev. *9*, 637–671.
7. Xie, S., Kaiser, D., and Cichy, R.M. (2020). Visual Imagery and Perception Share Neural Representations in the Alpha Frequency Band. Curr. Biol. *30*, 3062.
8. Foster, J.J., Sutterer, D.W., Serences, J.T., Vogel, E.K., and Awh, E. (2016). The topography of alpha-band activity tracks the content of spatial working memory. J. Neurophysiol. *115*, 168–177.
9. Foster, J.J., Bsales, E.M., Jaffe, R.J., and Awh, E. (2017). Alpha-band activity reveals spontaneous representations of spatial position in visual working memory. Curr. Biol. *27*, 3216–3223.e6.
10. Sutterer, D.W., Foster, J.J., Serences, J.T., Vogel, E.K., and Awh, E. (2019). Alpha-band oscillations track the retrieval of precise spatial representations from long-term memory. J. Neurophysiol. *122*, 539–551.
11. Yu, Q., Teng, C., and Postle, B.R. (2020). Different states of priority recruit different neural representations in visual working memory. PLoS Biol. *18*, e3000769.
12. Rose, N.S., LaRocque, J.J., Riggall, A.C., Gosseries, O., Starrett, M.J., Meyering, E.E., and Postle, B.R. (2016). Reactivation of latent working memories with transcranial magnetic stimulation. Science *354*, 1136–1139.
13. Miyake, A., and Friedman, N.P. (2012). The nature and organization of individual differences in executive functions: Four general conclusions. Curr. Dir. Psychol. Sci. *21*, 8–14.
14. Oberauer, K., Lewandowsky, S., Awh, E., Brown, G.D.A., Conway, A., Cowan, N., Donkin, C., Farrell, S., Hitch, G.J., Hurlstone, M.J., et al. (2018). Benchmarks for models of short-term and working memory. Psychol. Bull. *144*, 885–958.
15. D'Esposito, M., Postle, B.R., Ballard, D., and Lease, J. (1999). Maintenance versus manipulation of information held in working memory: an event-related fMRI study. Brain Cogn. *41*, 66–86.
16. Glahn, D.C., Kim, J., Cohen, M.S., Poutanen, V.P., Therman, S., Bava, S., Van Erp, T.G.M., Manninen, M., Huttunen, M., Lönnqvist, J., et al. (2002). Maintenance and manipulation in spatial working memory: dissociations in the prefrontal cortex. Neuroimage *17*, 201–213.
17. Veltman, D.J., Rombouts, S.A., and Dolan, R.J. (2003). Maintenance versus manipulation in verbal working memory revisited: an fMRI study. Neuroimage *18*, 247–256.
18. Jordan, K., Heinze, H.-J., Lutz, K., Kanowski, M., and Jäncke, L. (2001). Cortical activations during the mental rotation of different visual objects. Neuroimage *13*, 143–152.
19. Kaas, A., Weigelt, S., Roebroeck, A., Kohler, A., and Muckli, L. (2010). Imagery of a moving object: the role of occipital cortex and human MT/V5+. Neuroimage *49*, 794–804.
20. Klein, I., Paradis, A.-L., Poline, J.-B., Kosslyn, S.M., and Le Bihan, D. (2000). Transient activity in the human calcarine cortex during visual-mental imagery: an event-related fMRI study. J. Cogn. Neurosci. *12*, 15–23.
21. Knauff, M., Kassubek, J., Mulack, T., and Greenlee, M.W. (2000). Cortical activation evoked by visual mental imagery as measured by fMRI. Neuroreport *11*, 3957–3962.
22. Koenigs, M., Barbey, A.K., Postle, B.R., and Grafman, J. (2009). Superior parietal cortex is critical for the manipulation of information in working memory. J. Neurosci. *29*, 14980–14986.
23. Richter, W., Somorjai, R., Summers, R., Jarmasz, M., Menon, R.S., Gati, J.S., Georgopoulos, A.P., Tegeler, C., Ugurbil, K., and Kim, S.-G. (2000). Motor area activity during mental rotation studied by time-resolved single-trial fMRI. J. Cogn. Neurosci. *12*, 310–320.
24. Albers, A.M., Kok, P., Toni, I., Dijkerman, H.C., and de Lange, F.P. (2013). Shared Representations for Working Memory and Mental Imagery in Early Visual Cortex. Curr. Biol. *23*, 1427–1431.
25. Christophel, T.B., Cichy, R.M., Hebart, M.N., and Haynes, J.-D. (2015). Parietal and early visual cortices encode working memory content across mental transformations. Neuroimage *106*, 198–206.
26. Carlesimo, G.A., Perri, R., Turriziani, P., Tomaiuolo, F., and Caltagirone, C. (2001). Remembering What But Not Where: Independence of Spatial and Visual Working Memory in the Human Brain. Cortex *37*, 519–534.
27. Farah, M.J., Hammond, K.M., Levine, D.N., and Calvanio, R. (1988). Visual and spatial mental imagery: Dissociable systems of representation. Cogn. Psychol. *20*, 439–462.
28. Hecker, R., and Mapperson, B. (1997). Dissociation of visual and spatial processing in working memory. Neuropsychologia *35*, 599–603.
29. Logie, R.H., and Marchetti, C. (1991). Visuo-spatial working memory: Visual, spatial or central executive? In Advances in psychology, R.H. Logie and M. Denis, eds. (Elsevier), pp. 105–115.
30. Luzzatti, C., Vecchi, T., Agazzi, D., Cesa-Bianchi, M., and Vergani, C. (1998). A neurological dissociation between preserved visual and impaired spatial processing in mental imagery. Cortex *34*, 461–469.
31. Mecklinger, A., and Pfeifer, E. (1996). Event-related potentials reveal topographical and temporal distinct neuronal activation patterns for spatial and object working memory. Brain Res. Cogn. Brain Res. *4*, 211–224.
32. Mohr, H.M., and Linden, D.E.J. (2005). Separation of the systems for color and spatial manipulation in working memory revealed by a dual-task procedure. J. Cogn. Neurosci. *17*, 355–366.
33. Smith, E.E., Jonides, J., Koeppe, R.A., Awh, E., Schumacher, E.H., and Minoshima, S. (1995). Spatial versus object working memory: PET investigations. J. Cogn. Neurosci. *7*, 337–356.
34. Vecchi, T., and Cornoldi, C. (1999). Passive storage and active manipulation in visuo-spatial working memory: Further evidence from the study of age differences. Eur. J. Cognit. Psychol. *11*, 391–406.
35. Vicari, S., Bellucci, S., and Carlesimo, G.A. (2006). Evidence from two genetic syndromes for the independence of spatial and visual working memory. Dev. Med. Child Neurol. *48*, 126–131.
36. Baldassano, C., Esteva, A., Fei-Fei, L., and Beck, D.M. (2016). Two distinct scene-processing networks connecting vision and memory. Eneuro *3*.
37. Breedlove, J.L., St-Yves, G., Olman, C.A., and Naselaris, T. (2020). Generative feedback explains distinct brain activity codes for seen and mental images. Curr. Biol. *30*, 2211–2224.e6.
38. Favila, S.E., Samide, R., Sweigart, S.C., and Kuhl, B.A. (2018). Parietal Representations of Stimulus Features Are Amplified during Memory Retrieval and Flexibly Aligned with Top-Down Goals. J. Neurosci. *38*, 7809–7821.
39. Favila, S.E., Lee, H., and Kuhl, B.A. (2020). Transforming the Concept of Memory Reactivation. Trends Neurosci. *43*, 939–950.
40. Xiao, X., Dong, Q., Gao, J., Men, W., Poldrack, R.A., and Xue, G. (2017). Transformed neural pattern reinstatement during episodic memory retrieval. J. Neurosci. *37*, 2986–2998.
41. Buchsbaum, B.R., Lemire-Rodger, S., Fang, C., and Abdi, H. (2012). The neural basis of vivid memory is patterned on perception. J. Cogn. Neurosci. *24*, 1867–1883.
42. Naselaris, T., Olman, C.A., Stansbury, D.E., Ugurbil, K., and Gallant, J.L. (2015). A voxel-wise encoding model for early visual areas decodes mental images of remembered scenes. Neuroimage *105*, 215–228.
43. Polyn, S.M., Natu, V.S., Cohen, J.D., and Norman, K.A. (2005). Category-specific

cortical activity precedes retrieval during memory search. Science *310*, 1963–1966.
44. Slotnick, S.D., Thompson, W.L., and Kosslyn, S.M. (2005). Visual mental imagery induces retinotopically organized activation of early visual areas. Cereb. Cortex *15*, 1570–1583.
45. van Loon, A.M., Olmos-Solis, K., Fahrenfort, J.J., and Olivers, C.N. (2018). Current and future goals are represented in opposite patterns in object-selective cortex. Elife *7*, e38677.
46. Lewis-Peacock, J.A., Cohen, J.D., and Norman, K.A. (2016). Neural evidence of the strategic choice between working memory and episodic memory in prospective remembering. Neuropsychologia *93*, 280–288.
47. Cohen, M.X. (2014). Analyzing Neural Time Series Data: Theory and Practice (MIT Press).
48. van Moorselaar, D., Foster, J.J., Sutterer, D.W., Theeuwes, J., Olivers, C.N.L., and Awh, E. (2018). Spatially selective alpha oscillations reveal moment-by-moment trade-offs between working memory and attention. J. Cogn. Neurosci. *30*, 256–266.
49. Bae, G.-Y., and Luck, S.J. (2018). Dissociable Decoding of Spatial Attention and Working Memory from EEG Oscillations and Sustained Potentials. J. Neurosci. *38*, 409–422.
50. Awh, E., and Jonides, J. (2001). Overlapping mechanisms of attention and spatial working memory. Trends Cogn. Sci. *5*, 119–126.
51. Gazzaley, A., and Nobre, A.C. (2012). Top-down modulation: bridging selective attention and working memory. Trends Cogn. Sci. *16*, 129–135.
52. Kiyonaga, A., and Egner, T. (2013). Working memory as internal attention: Toward an integrative account of internal and external selection processes. Psychon. Bull. Rev. *20*, 228–242.
53. Postle, B.R. (2006). Working memory as an emergent property of the mind and brain. Neuroscience *139*, 23–38.
54. Hakim, N., Adam, K.C., Gunseli, E., Awh, E., and Vogel, E.K. (2019). Dissecting the neural focus of attention reveals distinct processes for spatial attention and object-based storage in visual working memory. Psychol. Sci. *30*, 526–540.
55. van Driel, J., Gunseli, E., Meeter, M., and Olivers, C.N.L. (2017). Local and interregional alpha EEG dynamics dissociate between memory for search and memory for recognition. Neuroimage *149*, 114–128.
56. Günseli, E., Fahrenfort, J.J., van Moorselaar, D., Daoultzis, K.C., Meeter, M., and Olivers, C.N.L. (2019). EEG dynamics reveal a dissociation between storage and selective attention within working memory. Sci. Rep. *9*, 13499.
57. Ataseven, N., Todorova, L., Yucel, D., Güler, B., Fukuda, K., and Gunseli, E. (2022). Individual differences in working memory reactivation of long-term memories predict protection against anticipated interference. Preprint at PsyArXiv *10*.
58. Şentürk, Y.D., Ünver, N., Demircan, C., Egner, T., and Günseli, E. (2023). The reactivation of task rules triggers the reactivation of task-relevant items. Cortex *171*, 465–480.
59. Brainard, D.H., and Vision, S. (1997). The psychophysics toolbox. Spat. Vis. *10*, 433–436.
60. Lins, O.G., Picton, T.W., Berg, P., and Scherg, M. (1993). Ocular artifacts in EEG and event-related potentials I: Scalp topography. Brain Topogr. *6*, 51–63.
61. Oostenveld, R., Fries, P., Maris, E., and Schoffelen, J.-M. (2011). FieldTrip: open source software for advanced analysis of MEG, EEG, and invasive electrophysiological data. Comput. Intell. Neurosci. *2011*, 156869.
62. Maris, E., and Oostenveld, R. (2007). Nonparametric statistical testing of EEG-and MEG-data. J. Neurosci. Methods *164*, 177–190.

STAR★METHODS

KEY RESOURCES TABLE

REAGENT or RESOURCE	SOURCE	IDENTIFIER
Deposited data		
Raw data and MATLAB code	Open Science Framework	https://osf.io/rvz39/
Experimental models: Organisms/strains		
Fifty-six healthy human volunteers participated in the study. Fourth-eight datasets left after exclusion (mean age = 23.12, 24 female)	N/A	N/A
Software and algorithms		
MATLAB	Mathworks	https://www.mathworks.com/products/matlab.html
Psychtoolbox	The Psychophysics Toolbox	http://psychtoolbox.org/
JASP	JASP Team (2023).	https://jasp-stats.org/

RESOURCE AVAILABILITY

Lead contact

Further information and requests for resources should be directed to the lead contact, Eren Günseli (gunseli.eren@gmail.com).

Materials availability

This study did not generate new materials.

Data and code availability

- The EEG data used in the study were collected by the experimenters using a custom code experiment file on MATLAB Psychtoolbox.[59]
- All data are available on the Open Science Framework platform (Data: https://osf.io/rvz39/).
- All codes are available on the Open Science Framework platform (Code: https://osf.io/rvz39/).

EXPERIMENTAL MODEL AND STUDY PARTICIPANT DETAILS

Fifty-six healthy volunteers participated in the experiments for monetary compensation ($15/h), 37 in Experiment 1 and 19 in Experiment 2. The target number of subjects for Experiment 2 was determined based on a downsampling procedure using the data from Experiment 1 that tested how many data points were required to observe a significant CTF slope for the updated location during the second retention interval (see design and procedure). Subjects reported normal or corrected-to-normal vision and provided informed consent according to procedures approved by the University of Chicago Institutional Review Board. Subjects were excluded from analysis if, after artifact rejection, they had less than 75 trials per angular location for either the encoded position or the updated position (seven in Experiment 1, zero in Experiment 2). One additional subject was excluded from the analysis in Experiment 2 because of an interrupted communication between the stimulus presentation computer and the EEG recording computer. In addition to the numbers provided above, in Experiment 2, 4 volunteers did not complete data collection (one battery died, two dropped out, one the eye tracker could not track eyes). Thus, the analysis included 30 subjects in Experiment 1 (age *Mean* = 23.2 *Standard deviation* = 4.1; 17 male) and 18 subjects in Experiment 2 (age M = 23, SD = 3.7; 7 male).

METHOD DETAILS

Stimuli

Stimuli were generated in MATLAB (Mathworks) using the Psychophysics Toolbox (Brainard 1997; Pelli 1997) and were presented on a 24-in. LCD monitor (refresh rate: 120 Hz). Viewing distance was ~100 cm in Experiment 1 and ~75 cm in Experiment 2. Figure 1 shows an example trial. The background color was gray (22.5 Cd/m^2). Throughout the trial, there was a black fixation circle (0.8 Cd/m^2; radius ~0.1° visual angle) at the center of the screen. Throughout the trial except for the sample display, five dark gray placeholders (9.8 Cd/m^2; radius 0.8° in Experiment 1, radius 1.1° in Experiment 2) were presented centered equidistantly on an imaginary circle (radius 3° in Experiment 1, radius 5° in Experiment 2). During the sample display, one of the placeholders was replaced by a red circle (15.5 Cd/m^2; radius 0.8° in Experiment 1, radius 1.1° in Experiment 2) that indicated the memory location. At the test display, there were light gray rings (43.9 Cd/m^2; thickness

~0.1°) around the placeholders. At the feedback screen, the outline of the placeholder that the subject selected was presented in white (124.7 Cd/m^2) and the placeholder that contained the correct updated position was filled in red as it was in the memory display. Additionally, during the feedback screen in Experiment 2 the accuracy of response was verbally indicated (i.e., "Correct", "Wrong", "You did not fixate on any placeholder").

The sound files for the update cue were created using Adobe Audition (http://www.adobe.com). The update cue was played through earphones (ER-3C audiometric earphone 10 Ω, www.etymotic.com). The tones were 175 Hz, 440 Hz, and 1109 Hz for the counterclockwise move, stay, and clockwise move, respectively. These frequencies correspond to notes in Western music that divide the octave into three equal steps. The single tones, which indicated a one-step movement, were normalized according to the equal-loudness contour. For two-step update cues, the middle of the tone was replaced with 80 ms of silence resulting in a double tone. All sound files were 220 ms. Single tones, which indicate a one-step update, have signal throughout the file, while double tones consist of two 70 ms signals interleaved with an 80 ms of silence in between. All sound files had 5 ms ramps at the beginning and end of the files to prevent artifacts during playback. In Experiment 2, each frequency was played in a different timbre (guitar for low, piano for mid, and flute for high frequency) to increase discriminability.

Design and procedure

Subjects initiated each trial by pressing the space bar. The fixation circle was presented for a randomly sampled duration between 600 and 1000 ms. Next, the memory display was presented for 250 ms in Experiment 1 and 150 ms in Experiment 2. Following the initial retention interval of 500 ms, the update cue was played through earphones for 220 ms during which the visual display was the same as the rest of the retention interval. After a second retention interval of 1500 ms in Experiment 1 and 1000 ms in Experiment 2, the test display was presented until response or an upper limit of 4000 ms. Following the response or 4000 ms, the feedback screen was presented for 1000 ms in Experiment 1 and 500 ms in Experiment 2. At the end of each block, written feedback was provided that indicated the block average accuracy in Experiment 1, and block average accuracy and RT in Experiment 2. In Experiment 2, the trial was aborted, and written feedback was presented for 500 ms if there was an ocular artifact during the trial. The ocular artifact feedback told the subject that they moved their eyes too early (i.e., before the test display) or blinked their eyes.

Subjects were instructed to remember the encoded position until the update cue and to update the position in their mind to the location indicated by the update cue as fast as possible following the cue. They were also told to hold the updated position in mind until the test display. In Experiment 1, the task was to use the mouse to click on the placeholder that contained the updated position as indicated by the update cue. In Experiment 2, subjects made the response by gaze position instead of a mouse click. Specifically, they were told to move their eyes to the placeholder that they thought contained the updated position as fast as possible without risking accuracy. For both experiments, subjects were instructed to maintain fixation from the beginning of the trial until the onset of the test display.

At the beginning of each experiment, there was a cue familiarization phase of 50 trials at which subjects passively viewed the presentation of the encoded position, and following the audio play of the update cue the presentation of the updated position. This was to ensure that subjects learned the relationship between each tone and its meaning. After the cue familiarization, subjects performed a practice phase of 50 trials which were identical to the real experiment. The real experiment consisted of 16 blocks of 50 trials in Experiment 1 and 12 blocks of 125 trials in Experiment 2. Encoded and updated positions were counterbalanced using a full factorial design within each block. That is, each combination of the encoded position and the updated position was equally presented. After artifact rejection, the average number of trials used in analyses was 594.9 (*SD* = 91.9) in Experiment 1 and 1304.2 (*SD* = 147.5) in Experiment 2.

EEG recording

We recorded EEG activity using 30 active Ag/AgCl electrodes mounted in an elastic cap (Brain Products actiCHamp, Munich, Germany). We recorded from International 10–20 sites: FP1, FP2, F7, F3, Fz, F4, F8, FC5, FC1, FC2, FC6, C3, Cz, C4, CP5, CP1, CP2, CP6, P7, P3, Pz, P4, P8, PO7, PO3, PO4, PO8, O1, Oz, and O2. Two additional electrodes were placed on the left and right mastoids, and a ground electrode was placed at position FPz. All sites were recorded with the left-mastoid reference and were re-referenced offline to the algebraic average of the left and right mastoids. Electrophysiological signals were filtered (low cut-off = 0.01 Hz, high cut-off = 80 Hz, slope from low-to high-cutoff = 12 dB/octave) and recorded with a 500 Hz sampling rate. Impedance values were kept below 15 kΩ. Eye movements and blinks were monitored using EOG, recorded with passive Ag/AgCl electrodes. Horizontal EOG was recorded from a bipolar pair of electrodes placed ~1 cm lateral to the external canthi. Vertical EOG was recorded from a bipolar pair of electrodes placed ~2 cm above and below the right eye.

QUANTIFICATION AND STATISTICAL ANALYSIS

Behavioral

Only trials with accurate responses were used for reaction time (RT) analysis. For the investigation of the relationship between behavioral and EEG measures, only artifact-free EEG trials were used to match the trials that are used to calculate behavioral and EEG scores.

Eye-tracking

Gaze position was monitored using a desk-mounted infrared eye-tracking system (EyeLink 1000 Plus, SR Research, Ontario, Canada), operating in the remote mode in Experiment 1 and the chin-rest mode in Experiment 2. According to the manufacturer, this system provides a

spatial resolution of 0.01° and an average accuracy of 0.25–0.5°. The gaze position was sampled at 500 Hz. We obtained usable eye-tracking data for 26 out of 30 subjects in Experiment 1.

In Experiment 2, the behavioral response was made by ocular position. Therefore, the experiment was aborted for one subject whose eye tracker data was not stable. All the remaining subjects had usable eye-tracking data. In Experiment 2, online feedback regarding ocular artifacts was provided. Trials were aborted if the eyes deviated away from the fixation by 1.6° visual degrees from the sample display until the test display. This threshold was adjusted during data collection based on the eye tracker data quality to optimize ocular artifact detection. For unstable gaze data, the threshold was increased to detect as many real eye movements as possible and to minimize unnecessary trial abortions due to eye tracker noise. Whereas, for stable gaze data the threshold was decreased to detect as many eye movements as possible.

In Experiment 2, the responses were registered via gaze position recording during the test display. At the test display, subjects moved their eyes to the placeholder that they thought contained the updated position. A response was registered if the average gaze position of both eyes were within an imaginary radius of 1.6° visual degrees around the center of any placeholder. This threshold, similar to the ocular artifact threshold, was adjusted during data collection based on the quality of the eye tracker data to maximize accurate response registration.

Artifact rejection

The artifact rejection was performed by visual inspection of the EEG signal for recording artifacts (blocking, muscle noise, and skin potentials), and the EOG signal and eye-tracking data (for those subjects with usable eye-tracking data) for ocular artifacts (blinks and eye movements). The threshold for ocular artifacts was optimized for each subject to remove as many real ocular artifacts as possible while reducing false alarms to account for noisy EOG and eye tracking signal. Our starting point was 20 μV in the HEOG corresponding to less than 1 visual degrees[60] and 0.5 visual degrees in the eye tracker. Trials with an inaccurate response were excluded from all EEG analysis except the investigation of the relationship between EEG and response accuracy.

Power analyses

Power analyses were performed using MATLAB's Signal Processing toolbox (Mathworks, Natick, MA), EEGLAB toolbox (Delorme & Makeig, 2004), and FieldTrip toolbox (Oostenveld et al., 2011). To isolate frequency-specific activity at each electrode, the raw EEG signal was bandpass filtered using a Butterworth filter as implemented by the ft_preproc_bandpassfilter.m function of FieldTrip Toolbox.[61] A Hilbert Transform (MATLAB Signal Processing Toolbox) was applied to the bandpass-filtered data, to extract a complex analytic signal, $z(t) = f(t) + i\tilde{f}(t)$, of the band-pass filtered EEG, $f(t)$, where $\tilde{f}(t)$ is the Hilbert Transform of $f(t)$ and $i = \sqrt{-1}$, using the following MATLAB syntax:

$$\text{hilbert}(\text{ft\_preproc\_bandpassfilter}\ (\text{data}, \text{F}, [\text{f1}, \text{f2}])')'$$

where data is the raw EEG (trials x samples), F is the sampling frequency (500 Hz), f1 and f2 are the boundaries of the frequency band to be isolated. For the time-frequency analysis, we f1 and f2 spanned across 4 Hz–50 Hz in increments of 2 Hz with a 2-Hz bandpass: f1 and f2 were 4 and 6 to isolate 4- to 6-Hz activity; 6 and 8 to isolate 6- to 8-Hz activity; and so on. For alpha-band analyses, f1 and f2 were 8 and 12 Hz, respectively.

Inverted encoding model of spatial position

Reconstructing the content of spatial WM

Following Foster et al. (2016), we used an IEM to reconstruct spatially selective CTFs from the scalp distribution of total power across electrodes. We assumed that power measured at each electrode reflects the weighted sum of five spatial channels (i.e., neuronal populations), each tuned for a different angular location (cf. Foster et al., 2016). We modeled the response profile of each spatial channel across angular location bins as a half sinusoid raised to the seventh power, given by:

$$R = \sin(0.5\theta)^7$$

where θ is the angular location (ranging from 0° to 359°), and R is the response of the spatial channel in arbitrary units. This response profile was circularly shifted for each channel such that the peak response of each spatial channel was centered over one of the five positions corresponding to the placeholder positions (0°, 72°, 144°, 216°, 288°, see Figure 1).

An IEM routine was applied to each time point. This routine proceeded in two stages (train and test). In the training stage, training data B_1 were used to estimate weights that approximate the relative contribution of the five spatial channels to the observed response measured at each electrode. Let B_1 (m electrodes × n_1 observations) be the power at each electrode for each measurement in the training set, C_1 (k channels × n_1 observations) be the predicted response of each spatial channel (determined by the basis functions) for each measurement, and W (m electrodes × k channels) be a weight matrix that characterizes a linear mapping from "channel space" to "electrode space". The relationship between B_1, C_1, and W can be described by a general linear model of the form:

$$B_1 = WC_1$$

The weight matrix was obtained via least-squares estimation as follows:

$$\widehat{W} = B_1 C_1^T \left(C_1 C_1^T\right)^{-1}$$

In the test stage, with the weights in hand, we inverted the model to transform the observed test data B_2 (m electrodes × n_2 observations) into estimated channel responses, C_2 (k channels × n_2 observations):

$$\widehat{C_2} = \left(\widehat{W}^T \widehat{W}\right)^{-1} \widehat{W}^T B_2$$

Each estimated channel response function was circularly shifted to a common center (i.e., 0° on the "Channel Offset" axes of the plots in Figure 2) by aligning the estimated channel responses to the channel tuned for the stimulus location to yield CTFs. The IEM routine was performed separately for each time point.

We used a "leave-one-out" cross-validation routine such that two blocks of estimated power values (see Alpha-Band Power Analysis) served as B_1 and were used to estimate $\widehat{W}$, and the remaining block served as B_2 and was used to estimate C_2, ensuring that the training and test data were always independent. This process was repeated until each of the three blocks were held out as the test set, and the resulting CTFs were averaged across each test block. This IEM routine was applied separately for each subject, and statistical analyses were performed on the reconstructed CTFs.

To prevent bias in our analysis, we equated the number of observations across position bins within each block. Specifically, we calculated the minimum number of trials for any given position bin n for each subject and assigned $n/3$ many trials for each position bin to each of the three blocks. Importantly, the blocks were independent (i.e., no trial was repeated across blocks) to prevent circularity in the cross-validation procedures used for the IEM routine (see Forward Encoding Model). Total power was then calculated for each position bin for each block, resulting in a $p*b$ × m × s matrix, where p is the number of position bins, b is the number of blocks, m is the number of electrodes, and s is the number of time samples.

Finally, because we equated the number of trials across position bins within blocks, a random subset of trials was not included in any block. We randomly generated 30 block assignments each resulting in a $p*b$ × m × s power matrix. The IEM routine was applied to the matrices of power values for each block assignment, and their outputs (i.e., channel response profiles) were averaged. This iterative approach better utilized the complete dataset for each subject and reduces noise in the resulting CTFs by minimizing the influence of idiosyncrasies in estimates of power specific to any given assignment of trials to blocks.

Testing the representational similarity between the WM content for updated and encoded positions

The IEM analysis described above enabled testing whether there is location-selective information in the EEG signal for a given time point, separately for the encoded position and the updated position. To test whether the storage of the encoded content and the updated content share an overlapping representational space, we performed the aforementioned IEM with the following difference: We trained an IEM for the encoded position using data averaged across a pre-cue time and tested the IEM for the updated position for each time point.

To determine the time to be used for training the IEM, first, we ran a cross-temporal IEM for the encoded position until the cue onset. The CTF slope for this IEM was then visually inspected to assess how long it took for the CTF, thus the WM representation, to stabilize. Based on visual inspection, we decided that the CTF slope was stabilized after ~300 ms for both experiments (see Figure S4). In order to minimize the contamination in the EEG signal caused by mental updating, we set the end of the training time window to be 50 ms before the onset of the update cue. Thus, we trained the IEM on the encoded position using the alpha-band power averaged from 300 ms till 700 ms in Experiment 1, and from 300 ms till 600 ms in Experiment 2. Then, we tested the IEM on the updated position at each time point.

The model was blind to the updated location information since it was trained on the encoded position using data before the update cue. Therefore, we hypothesized that this analysis would reveal location-selective information for the updated position only if the storage of the *updated* WM content relies on an alpha-band power topography that is similar to the storage of the *encoded*, pre-updated WM content.

Statistical analysis

To quantify the location selectivity of the CTFs we estimated the CTF slope (i.e., the "peakedness" of the channel response at channel offset zero relative to farther channel offsets). CTF slope was estimated using linear regression by collapsing the channel responses across channels that were equidistant. To test whether the CTF slope was statistically above chance, we tested whether the CTF slope was different from zero using a one-sample t-test (two-tailed). Because the mean CTF slope may not be normally distributed under the null hypothesis, we employed a Monte Carlo randomization procedure to empirically approximate the null distribution of the t-statistic.

Specifically, we implemented an IEM by randomizing the location labels within each block so that the labels were random with respect to the observed EEG signal in each electrode. This randomization procedure was repeated 1,000 times to obtain a null distribution. CTF slope at each time point was compared against this null distribution using a two-tailed t-test.

Multiple comparisons correction was established using cluster-based permutation testing. First, a difference score was calculated by subtracting the surrogate null distribution from the real CTF slopes and this difference score was tested against zero using a two-sample t-test. Four or more temporally adjacent data points with a p value smaller than 0.05 were clustered together. Then, signs of the difference scores were randomly shuffled across participants 1,000 iterations. At each iteration, t-tests were performed on shuffled data. A cluster-level statistic was calculated by taking the sum of the t-values within each cluster, separately for positive and negative clusters. The p value for each cluster

was calculated as the number of times the sum of the absolute t-values within the cluster under random shuffling exceeds that of the t-values within the observed cluster. A cluster was considered significant if the calculated p value was smaller than 0.05. This approach corrects for multiple comparisons by taking into account clusters of modulations in data that can be expected by chance.[62]

The same approach was used for the statistical analyses of IEM across multiple frequency bands, ranging from 4 Hz to 50 Hz (4–6 Hz, 6–8 Hz, … 48–50 Hz), except that this time we downsampled the data to 50 Hz (i.e., one sample every 20 ms) prior to statistical analyses to reduce the computation time.

EEG-behavior relationship

To test whether the location selectivity of the CTF for the updated WM content predicts behavior, in Experiment 1 we looked at the correlation between the average CTF slope for the updated content following the update cue and the grand average accuracy and RT across subjects. For this analysis, we matched the trials used to calculate behavioral measures to the trials used to calculate CTF slopes by including only artifact-free trials. Also, we equated the number of trials across subjects to match the subject with the lowest number of trials to eliminate variance in mean CTF slope across subjects that is due to differences in EEG noise. Specifically, the number of trials in each position bin in each block was set to be 86 for the correlation with accuracy, and 76 for the correlation with RT, which was the minimum across subjects for all trials and correct response trials, respectively. Moreover, to capture the variability in RT for the updating of WM contents, we only included 'move' trials (i.e., excluded 'stay' trials) in this analysis.

In Experiment 2, the variability in RT was very low, but the number of artifact-free trials was more than twice that in Experiment 1. Thus, we investigated the CTF-behavior relationship across trials instead of across subjects. We applied a median-split on mean RT per subject and performed the standard IEM approach described above separately for the above-median RT and below-median RT trials. Like in Experiment 1, only correct-response and move trials were included in this analysis.

Eye bias control analysis

To test whether changes in EEG voltage that are due to eye movements account for the location selectivity in the EEG signal, we ran the main CTF analysis described above with the following differences. We performed this analysis for Experiment 2, in which there was reliable eye-tracking data for every participant and trial. The position bins were defined based on eye positions instead of the actual encoded and updated positions. The encoded position was defined as the location of the placeholder closest to the eye position averaged from the onset of the memory display until the onset of the update cue (i.e., 0–650 ms). The updated position was defined as the location of the placeholder closest to the eye position averaged from the offset of the update cue until the onset of the probe (i.e., 870–1870 ms).

Trials with noisy eye-tracking data were removed from this analysis resulting in fewer trials used compared to the main analysis, which resulted in the removal of only 1.06 trials on average (minimum 0, maximum 4 trials per subject). One subject who had less than 30 trials for a position bin in a 'block' of the CTF analysis was excluded from the analysis. Otherwise, the analysis was identical to our main analysis described above in reconstructing the content of spatial WM.

To ensure the validity of the comparison of the location selectivity across CTFs obtained based on WM location bins and eye position location bins, we performed the standard CTF analysis using the same subjects and trials used in the eye bias control analysis. If eye movements were responsible for the reconstruction of the updated position our main analysis, then using position labels based on eye positions should result in location selectivity.

To statistically confirm that eye bias is not responsible for the CTF location selectivity for encoded and updated positions, we compared the CTF slopes for encoded vs. updated positions separately for the CTF analyses that are based on actual positions and eye positions. We hypothesized that if eye movements do not underlie the location selectivity in the EEG signal, then a CTF slope difference between encoded and updated positions should be observed for actual position bins, but not eye-position-based bins.